# Characterisation of hydrocarbonaceous overlayers important in metal-catalysed selective hydrogenation reactions

David Lennon,[1] Robbie Warringham,[1] Tatiana Guidi[2] and Stewart F. Parker[2*]

1. School of Chemistry, Joseph Black Building, University of Glasgow, Glasgow G12 8QQ, UK.
2. ISIS Facility, STFC Rutherford Appleton Laboratory, Chilton, Didcot, Oxfordshire OX11 0QX, UK.

**Dedication**

Dedicated to Dr John Tomkinson and Dr Jerry Mayers on the occasion of their retirement.

*Author for correspondence
Dr Stewart F. Parker
ISIS Facility
STFC Rutherford Appleton Laboratory
Chilton
Didcot
Oxfordshire
OX11 0QX
UK.

Phone: +44 (0)1235 446182
Fax: +44 (0)1235 445720
Email: stewart.parker@stfc.ac.uk

**Abstract.**

The hydrogenation of alkynes to alkenes over supported metal catalysts is an important industrial process and it has been shown that hydrocarbonaceous overlayers are important in controlling selectivity profiles of metal-catalysed hydrogenation reactions. As a model system we have selected propyne hydrogenation over a commercial Pd(5%)/$Al_2O_3$ catalyst. Inelastic neutron scattering studies show that the C–H stretching mode ranges from 2850-3063 $cm^{-1}$, indicating the mostly aliphatic nature of the overlayer and this is supported by the quantification of the carbon and hydrogen on the surface. There is also a population of strongly hydrogen-bonded hydroxyls, their presence would indicate that the overlayer probably contains some oxygen functionality. There is little evidence for any olefinic or aromatic species. This is distinctly different from the overlayers that are deposited on Ni/$Al_2O_3$ catalysts during methane reforming that are largely graphitic in nature.

## 1. Introduction

The hydrogenation of alkynes to alkenes over supported metal catalysts is an important industrial process [1], *e.g.* in polyethylene manufacture where it is essential to remove the trace levels of ethyne present in the ethene feedstock to prevent runaway reactions [2]. Ethyne to ethene hydrogenation has been extensively studied and it has been shown that hydrocarbonaceous overlayers are important in controlling selectivity profiles of metal-catalysed hydrogenation reactions [3-5]. However, it has been suggested that ethyne is a special case rather than the norm [6].

The hydrogenation of higher alkynes has been much less studied, although it is clear that hydrocarbonaceous overlayers are also implicated in these cases as well [6-8]. While it is possible to quantify the carbon content by temperature programmed oxidation (TPO), the form and quantity of the hydrogen present is generally unknown, as the overlayer is invariably impervious to investigation by infrared spectroscopy. These lacunae were partly overcome in work from the Fritz Haber Institute on alkene hydrogenation over supported Pd nanoparticles [9]. The authors associate activity with adsorption states of hydrogen that are modified by carbonaceous deposits and have used $^{1}H$-($^{15}N,\alpha\gamma$)$^{12}C$ nuclear reaction analysis (NRA) for hydrogen depth profiling in order to monitor the adsorbed hydrogen. The work establishes a role

for hydrogen retention within the carbonaceous overlayer. Although this methodology can detect and quantify hydrogen retention, it is unable to define how the hydrogen is bound.

We have recently shown that vibrational spectroscopy with neutrons (inelastic neutron scattering, INS) is able to detect, speciate and quantify hydrogen in carbon deposited on nickel-alumina catalysts during methane reforming [10-12]. In the present paper we extend the methodology to investigate whether it is possible to better characterise the form of the hydrogen present in the hydrocarbonaceous overlayer that is an integral part of alkyne hydrogenation using supported metal catalysts.

## 2. Experimental

The catalyst samples were prepared in a gas rig developed [13] for the preparation of the large (10 – 20 g) samples required for INS spectroscopy. 10 g of a Pd(5%)/$Al_2O_3$ catalyst (Alfa Aesar) was loaded into an Inconel cell. The catalyst was activated by heating at 393 K in flowing He/$H_2$(10%) mixture. Propyne has a low vapour pressure at room temperature so was introduced into the gas manifold by entraining the vapour in a second helium stream. This was then mixed with the He/$H_2$(10%) stream and admitted to the reaction cell, which was maintained at 333 K. The reaction was continuously monitored by an on-line quadrupole mass spectrometer (MS, Spectra Microvision plus). The reaction was carried out for two to six hours and then stopped. The sample was then transferred in an argon glovebox to an indium sealed thin-walled aluminium can. The INS spectra were then recorded with various incident energies, $E_i$, using either MAPS [14] or MERLIN [15] at ISIS [16]. A sample that was activated but not reacted was used as the reference.

Post-reaction the carbon content was determined by temperature programmed oxidation (TPO). The studies were performed using a custom built reaction test rig consisting of ⅛ inch Swagelok tubing. Gas flows are controlled by Hastings Mass Flow controllers and are monitored by mass spectrometry using a Hiden HPR20 mass spectrometer. Samples were inserted into a quartz tube (4 mm internal diameter) and attached to the experimental rig using Cajun Ultra-Torr fittings. Sample heating was provided by a Eurotherm 3508 Microreactor oven. Approximately 40 mg of sample was heated to 1173 K at 5 K $min^{-1}$ under a flow of $O_2$ (5% $O_2$ in He, BOC Ltd, >99 %, 70 sccm). The resultant gases were measured by mass spectrometry analysing for the following

masses; m/z = 2, 4, 15, 18, 28, 32 and 44. Once the temperature ramp had completed, the sample was cooled under a flow of He (BOC Ltd, >99 %, 70 sccm).

### 3. Results and Discussion

As a model system we have selected propyne hydrogenation over a commercial $Pd(5\%)/Al_2O_3$ catalyst:

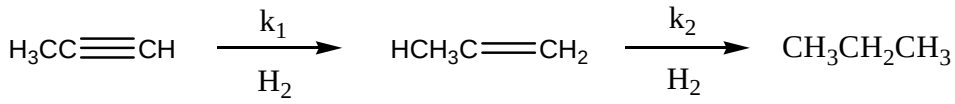


Robbie: please amend the scheme so that the middle is CH3CH=CH2

The reaction conforms to a consecutive process, with partial hydrogenation to propene ($k_1$) preceding full hydrogenation to propane ($k_2$) [7,8,17-19]. Figure 1 shows the on-line mass spectrometer output for the reaction. The immediate production of propene and propane demonstrates that this is a working catalyst. In addition to the expected hydrogenation products, propene and propane, there is also a significant production of the hydrogenolysis product ethene. This is not seen in microreactor studies [17-19] but probably arises because the space velocity in the large gas rig is only ~10% of that in the microreactor, so the residence time is much longer.

The INS spectrum (2500-4000 $cm^{-1}$) recorded using the MAPS spectrometer is shown in Figure 2. A feature assigned to hydroxyls on the alumina [11,12] is apparent, however, there is only a barely discernible feature (signal-to-noise ratio ~2) at 2970 $cm^{-1}$ in the region where a hydrocarbon signature would occur.

The spectrum shown in Figure 2 is disappointing, particularly in view of the fact that the catalysis was clearly occurring as seen in Figure 1. However, direct geometry instruments offer possibilities for trading between flux and resolution in a way that the more commonly used (for catalysis) indirect geometry instruments do not [14]. To increase the signal-to-noise ratio a threefold approach was adopted: (i) the reaction was run for six hours rather than two, (ii) MERLIN was used as the spectrometer since it is more sensitive than MAPS by virtue of a much larger solid angle of collection and the use of a guide on the incident beam [15] and (iii) a low resolution but high flux slit package was used in the Fermi chopper for energy selection.

Overall, the changes were expected to result in at least an order of magnitude improvement in sensitivity, albeit at significantly worse resolution.

Comparison of Figures 2 and 3 shows that these expectations have been met. The hydroxyl peak in Figure 2 has a full width at half maximum of ~360 $cm^{-1}$ whereas that in Figure 3a and 3b is ~400 $cm^{-1}$, since the peak is so broad the resolution would not be expected to change the width significantly. However, the sub-structure apparent in Figure 2, maxima at 3590 and 3700 $cm^{-1}$ which can be assigned to hydrogen bonded and isolated hydroxyls respectively, has disappeared and a single, asymmetric peak at 3600 $cm^{-1}$ is observed. The spectra in Figure 3a and 3b are normalised to the same mass of catalyst, thus it is apparent that ~50% of the hydroxyls have disappeared. Using Figure 3a as a reference spectrum, the remaining hydroxyls were subtracted from Figure 3b to give the scaled difference spectrum, 3c, (note that it is ×4 ordinate expanded relative to (a) and (b)). This may be curve resolved to show a feature at 2950 $cm^{-1}$ and a very broad feature at 3260 $cm^{-1}$.

The major difference between Figures 2 and 3 is that the signal-to-noise ratio is now ~10 for the peak at 2970 $cm^{-1}$ and it is now obviously present. The peak is asymmetric to the low energy side, suggesting that it is mostly aliphatic in origin, consistent with the weak feature seen in Figure 2.. This is supported by the observation of two peaks at 1365 and 1465 $cm^{-1}$ in Figure 4 that can be assigned to unresolved $CH_2$ twist and wag modes and $CH_2$ scissors respectively [20]. We note that the spectrum is markedly different from that of solid propyne [14], see Figure 5, and also from that of amorphous carbon [21].

The position of the broad feature at 3260 $cm^{-1}$ is consistent with the ≡C–H stretch of propyne, Figure 5, however, the other features that would be expected with adsorbed propyne are absent. In particular, the intense ≡C–H bend at 680 $cm^{-1}$ is not seen. Instead, a broad, weak feature at 990 $cm^{-1}$ is found. Together, the 3260 and 990 $cm^{-1}$ bands are consistent with the presence of strongly hydrogen-bonded hydroxyls. The transition energies are similar to those observed on alumina after reaction with HCl [22]. The downshift of the hydroxyls accounts, in part, for their apparent disappearance on reaction, Figure 3a, 3b.

The presence of the downshifted hydroxyls begs the question: to what are they hydrogen-

bonded? The only reasonable candidate is the hydrocarbonaceous overlayer that is formed during the reaction. This is mostly aliphatic in nature, thus the interaction would be similar to that between hydroxyls and alkanes. However, hydroxyls only form weak hydrogen bonds with alkanes, on a variety of oxides the O–H stretch modes are commonly found [23] in the range 3500 – 3600 $cm^{-1}$, downshifted only 100 $cm^{-1}$ or so from the free hydroxyl transition energy. This is much higher than is observed here. Stronger hydrogen bonds are formed between hydroxyls and alkenes, the downshift in the O–H stretch can be as much as 400 $cm^{-1}$ [24], however, this requires strong Brönsted acid sites and these are not observed on aluminas [25,26]. In addition, there is no evidence for the presence of $C(sp^2)$–H. The formation of strong hydrogen bonds requires the presence of strongly polar acceptors, thus we suggest that the overlayer must incorporate some oxygen functionality (presumably derived from the 'missing' hydroxyls) to account for the downshift. Unfortunately, the most likely functionality, carbonyl, is invisible to neutrons.

As noted earlier, we have shown that it is possible to quantify the hydrogen present on a catalyst by INS [11,12]. Figure 6 shows the INS spectrum of 0.5933 gm of polystyrene and the difference spectrum from 23.2 gm of catalyst in the beam. Using the methods described elsewhere [11,12] we calculate that there are 1.2 – 1.6 mg H $(g\ cat)^{-1}$ present on the catalyst surface. The range results from the uncertainty in the area of the peak at 2950 $cm^{-1}$ because of the presence of the hydroxyls. If these are curve fit as a single peak, as shown in Figure 3c, then the lower bound is obtained, if they are fit as two peaks, then the upper bound is obtained. The results of the TPO study are shown in Table 1 and combining the data, allows us to deduce a C:H ratio of 1:1.8 – 2.4. Thus the overlayer is essentially aliphatic in nature. This is distinctly different from the hydrocarbonaceous layer present on a $Ni/Al_2O_3$ methane reforming catalyst that has a C:H ratio in the range 160:1 to 2550:1 depending on the catalyst materials and preparation conditions [11,12].

## 4. Conclusions

The C–H stretching mode ranges from 2850-3063 $cm^{-1}$, indicating the mostly aliphatic nature of the overlayer and this is supported by the quantification of the carbon and hydrogen on the surface. There is also a population of strongly hydrogen-bonded hydroxyls, their presence would indicate that the overlayer probably contains some oxygen functionality. There is little evidence

for any olefinic or aromatic species. This is distinctly different from the overlayers that are deposited on $Ni/Al_2O_3$ catalysts during methane reforming that are largely graphitic in nature [10-12]. It is the hydrocarbonaceous overlayer that is believed to be controlling the hydrogen supply, which is then influencing the extent of hydrogenation [6].

The flexibility that is offered by the use of direct geometry instruments was crucial to the success of this work. Figure 3c represents a milestone and establishes that INS can be used to access important aspects of high specification heterogeneous catalysts.

**Acknowledgments**

We thank the STFC Rutherford Appleton Laboratory for access to neutron beam facilities.

**References**

[1] K. Wiessermel, H.-J. Arpe, Industrial Organic Chemistry, VCH, Weinheim, 1997, p. 63.

[2] A.J. Peacock, Handbook of Polyethylene – Structures, Properties and Applications, CRC Press, Baton Rouge, 2000.

[3] G. Webb, Catalysis Today, 7 (1990) 139.

[4] G.C. Bond, Appl. Catal. A 149 (1997) 3.

[5] B. Brandt, J.-H. Fischer, W. Ludwig, J. Libuda, F. Zaera, S. Schauermann, H.-J. Freund, J. Phys. Chem. C, 112 (2008) 11408.

[6] S.D. Jackson, G.J. Kelly, Curr. Top. Catal. 1 (1997) 47.

[7] D.R. Kennedy, G. Webb, S.D. Jackson, D. Lennon, Applied Catalysis A: General 259 (2004) 109–120.

[8] R. Marshall, G. Webb, S.D. Jackson, D. Lennon, Journal of Molecular Catalysis A: Chemical 226 (2005) 227–230.

[9] M. Wilde, K. Fukutani, W. Ludwig, B. Brandt, J.-H. Fischer, S. Schauermann, H.-J. Freund, Angew. Chem. Int. Ed., 47 (2008) 9289.

[10] I.P. Silverwood, N.G. Hamilton, J.Z. Staniforth, C.J. Laycock, S.F. Parker, R.M. Ormerod and D. Lennon, Catalysis Today, 155 (2010) 319–325.

[11] I.P. Silverwood, N.G. Hamilton, C.J. Laycock, J.Z. Staniforth, R.M. Ormerod, C.D. Frost, S.F. Parker and D. Lennon, Phys. Chem. Chem. Phys. 12 (2010) 3102-3107.

[12] I.P. Silverwood, N.G. Hamilton, A.R. McFarlane, J. Kapitán, L. Hecht, E. L. Norris, R. M. Ormerod, C.D. Frost, S.F. Parker and D. Lennon, Phys. Chem. Chem. Phys., 14 (2012) 15214-15225.

[13] I.P. Silverwood , N.G. Hamilton , A. McFarlane , R.M. Ormerod, T. Guidi, J. Bones, M.P. Dudman, C.M. Goodway, M. Kibble, S.F. Parker and D. Lennon, Rev. Sci. Inst., 82 (2011) 034101.

[14] S.F. Parker, D. Lennon and P.W. Albers, Appl. Spec. 65 (2011) 1325-1341.

[15] R.I. Bewley, R.S. Eccleston, K.A. McEwen, S.M. Hayden, M.T. Dove, S.M. Bennington, J.R. Treadgold, R.L.S. Coleman, Physica B 385-386 (2006) 1029-1031.

[16] www.isis.stfc.ac.uk

[17] D.R. Kennedy, B. Cullen, D. Lennon, G. Webb, P.R. Dennison and S.D. Jackson, Stud. Surf. Sci. Catal., 122 (1999) 125.

[18] D. Lennon, D.R. Kennedy, G. Webb and S.D. Jackson, Stud. Surf. Sci. Catal., 126 (1999) 341.

[19] D. Lennon, R. Marshall, G. Webb and S.D. Jackson, Stud. Surf. Sci. Catal., 130 (2000).

[20] D. Lin-Vien, N.B. Colthup, W.G. Fateley and J.G. Grasselli, Handbook of Infrared and Raman Characteristic Frequencies of Organic Molecules, Academic Press, Boston, 1991, ch. 1.

[21] P.W. Albers, J. Pietsch, J. Krauter and S.F. Parker, Phys. Chem. Chem. Phys., 5 (2003) 1941 - 1949.

[22] A.R. McInroy, D.T. Lundie, J.M. Winfield, C.C. Dudman, P. Jones, S.F. Parker and D. Lennon, Catalysis Today, 114 (2006) 403-411.

[23] A. Davydov, Molecular Spectroscopy of Oxide Catalyst Surfaces, Wiley, Chichester, 2003, ch. 5.4.

[24] G. Busca, V. Lorenzelli, G. Ramis, J. Saussey, J.C. Lavalley, J. Mol. Struct. 267 (1992) 315-329.

[25] A. Hess, E. Kemnitz, J. Catal. 149 (1994) 449-457.

[26] D.T. Lundie, A.R. McInroy, R. Marshall, J.M. Winfield, C. Mitchell, C.C. Dudman, P. Jones, S.F. Parker and D. Lennon, J. Phys. Chem. B, 109 (2005) 11592-11601.

Table 1: Carbon content of Pd(5%)/$Al_2O_3$ catalyst as a function of treatment as determined by temperature programmed oxidation.

| Sample | Carbon content / mg C $(g\ cat)^{-1}$ |
|---|---|
| Activated | 3.92 |
| Reacted (MAPS) | 4.88 |
| Reacted (MERLIN) | 7.86 |

**Figures**

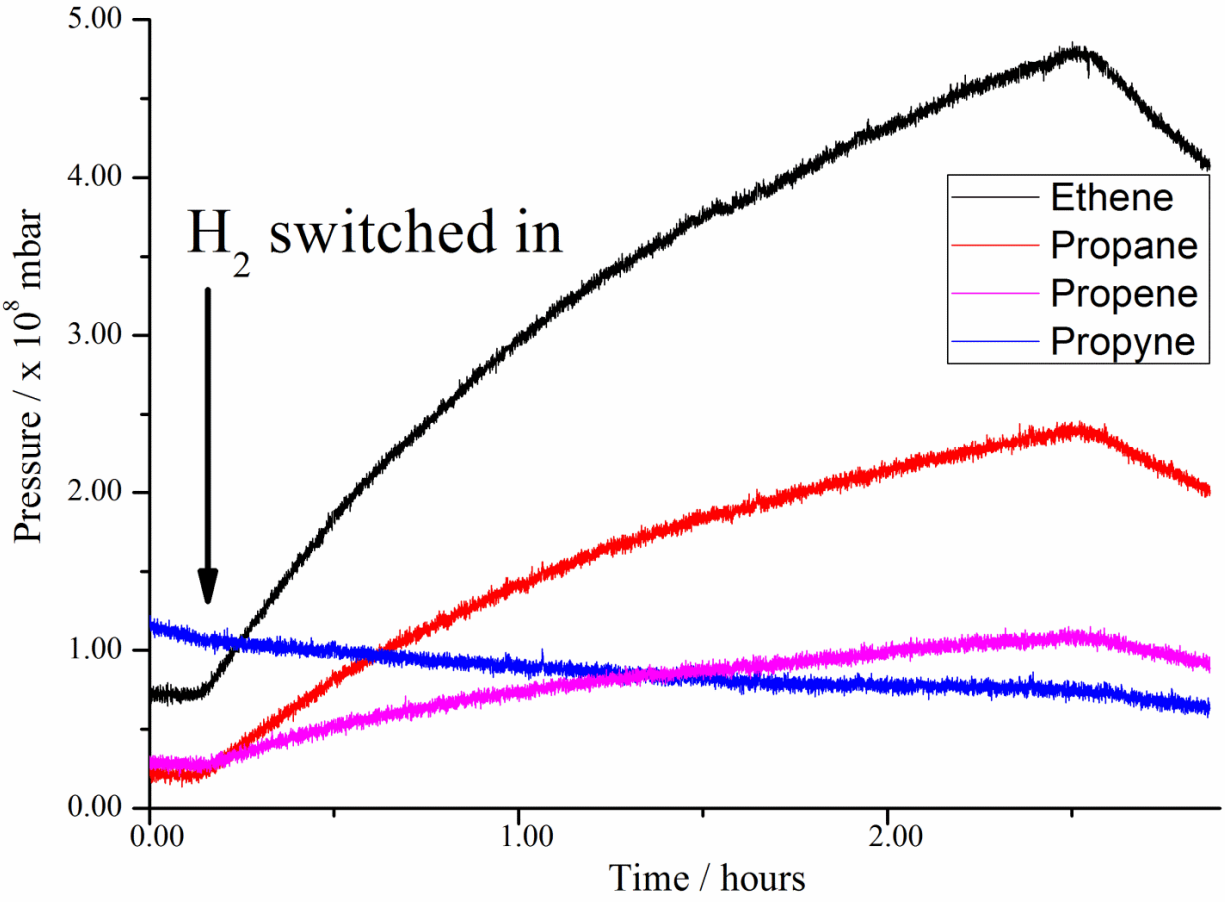


Figure 1. On-line mass spectrometer output for the hydrogenation of propyne over Pd(5%)/$Al_2O_3$.

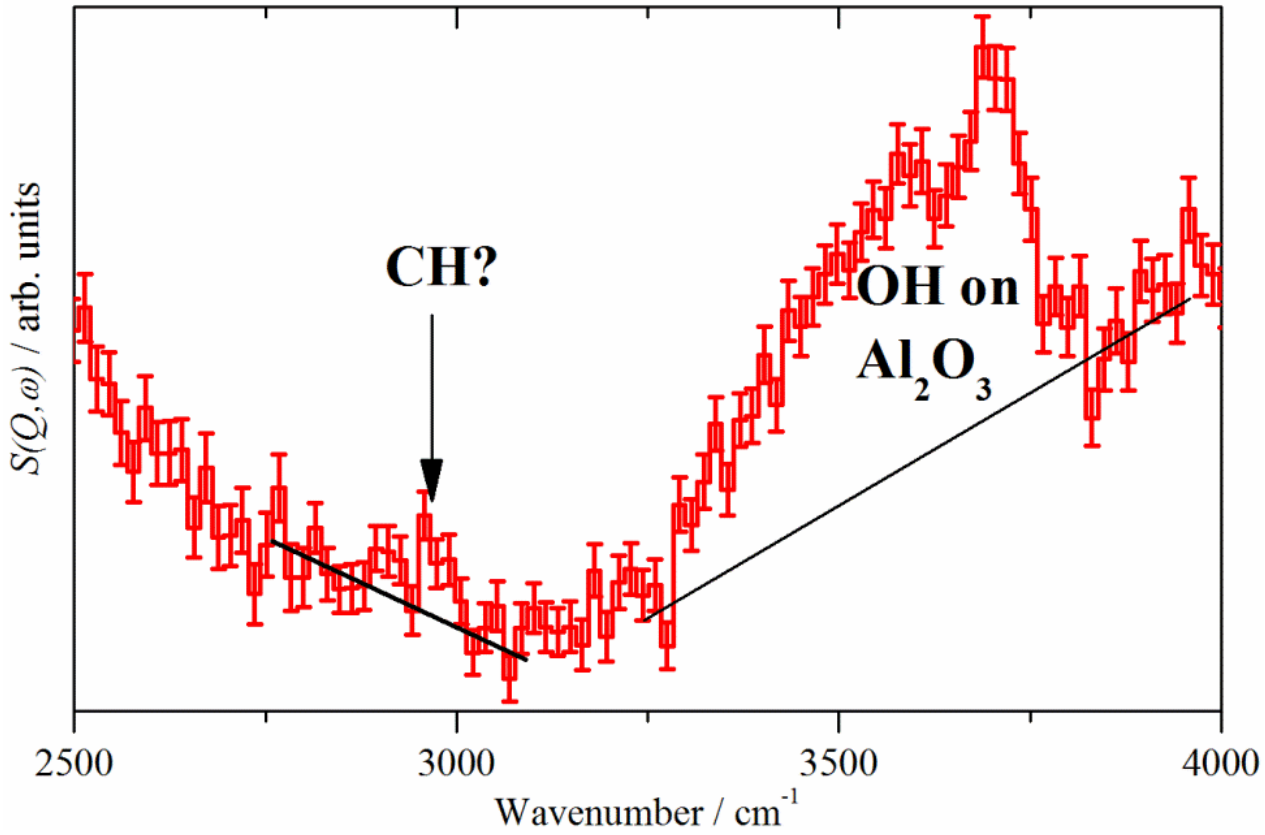


Figure 2. INS spectrum (recorded on MAPS with $E_i$ = 4840 $cm^{-1}$) of the Pd(5%)/$Al_2O_3$ catalyst after carrying out two hours of propyne hydrogenation reaction.

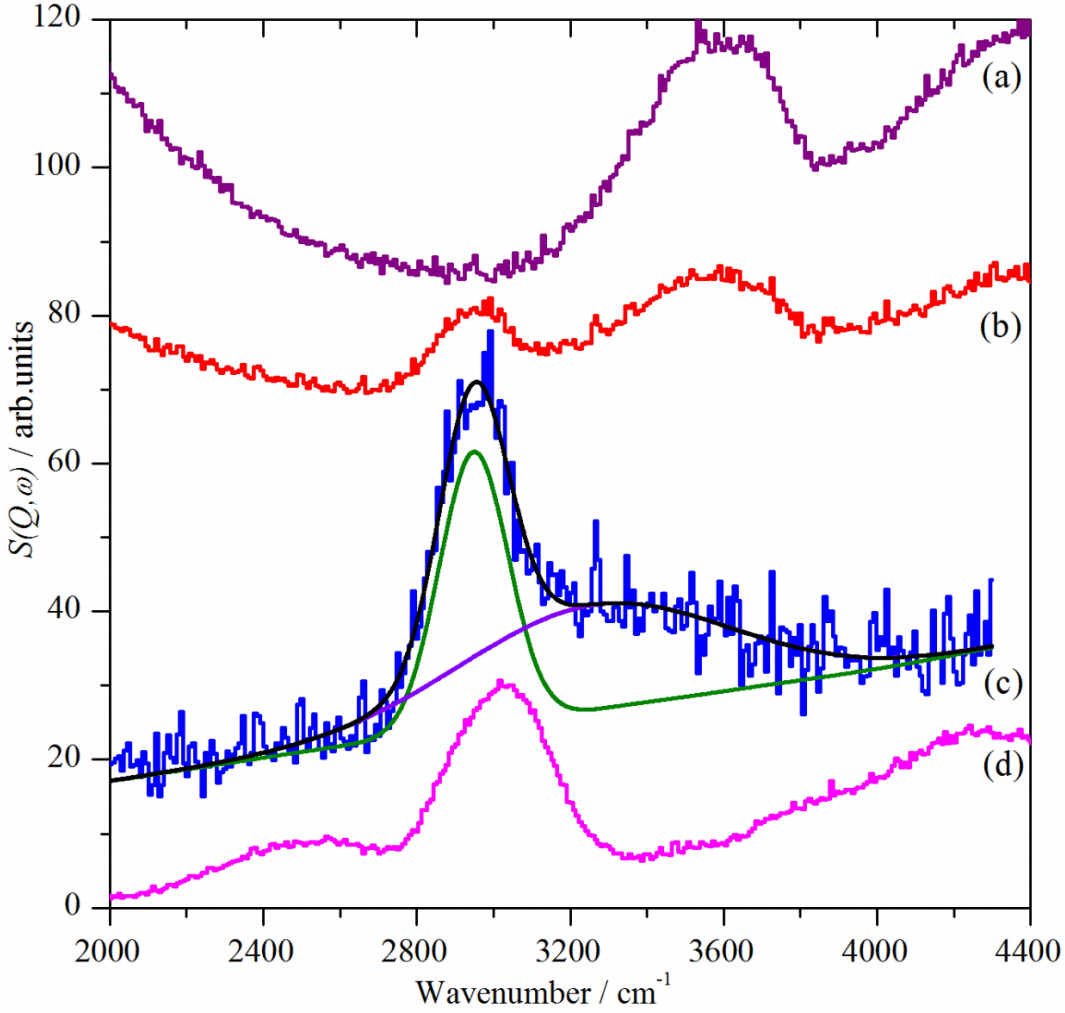


Figure 3. INS spectra (recorded on MERLIN with $E_i$ = 4840 $cm^{-1}$) of (a) the Pd(5%)/$Al_2O_3$ catalyst after activation, (b) the catalyst after carrying out six hours of the propyne hydrogenation reaction, (c) the scaled difference spectrum (×4 ordinate expanded relative to (a) and (b)) with curve resolved components and the total fit and (d) 0.5933 g of polystyrene (×0.5 ordinate expanded relative to (a) and (b)).

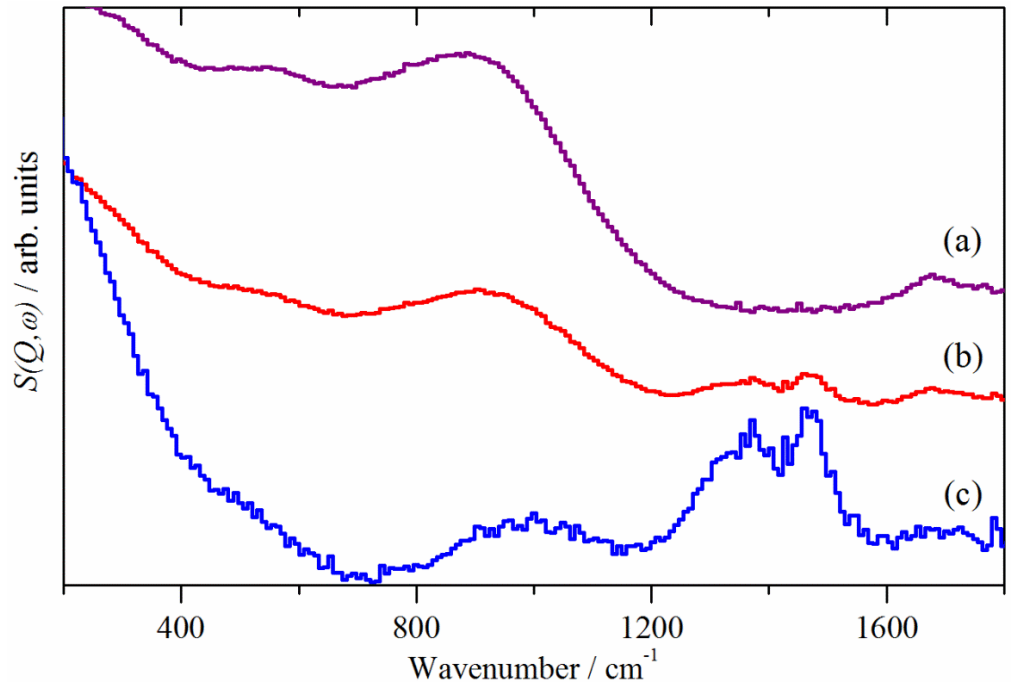


Figure 4. INS spectra (recorded on MERLIN with $E_i$ = 2017 $cm^{-1}$) of (a) the Pd(5%)/$Al_2O_3$ catalyst after activation, (b) the catalyst after carrying out six hours of the propyne hydrogenation reaction and (c) the scaled difference spectrum (×4 ordinate expanded relative to (a) and (b)).

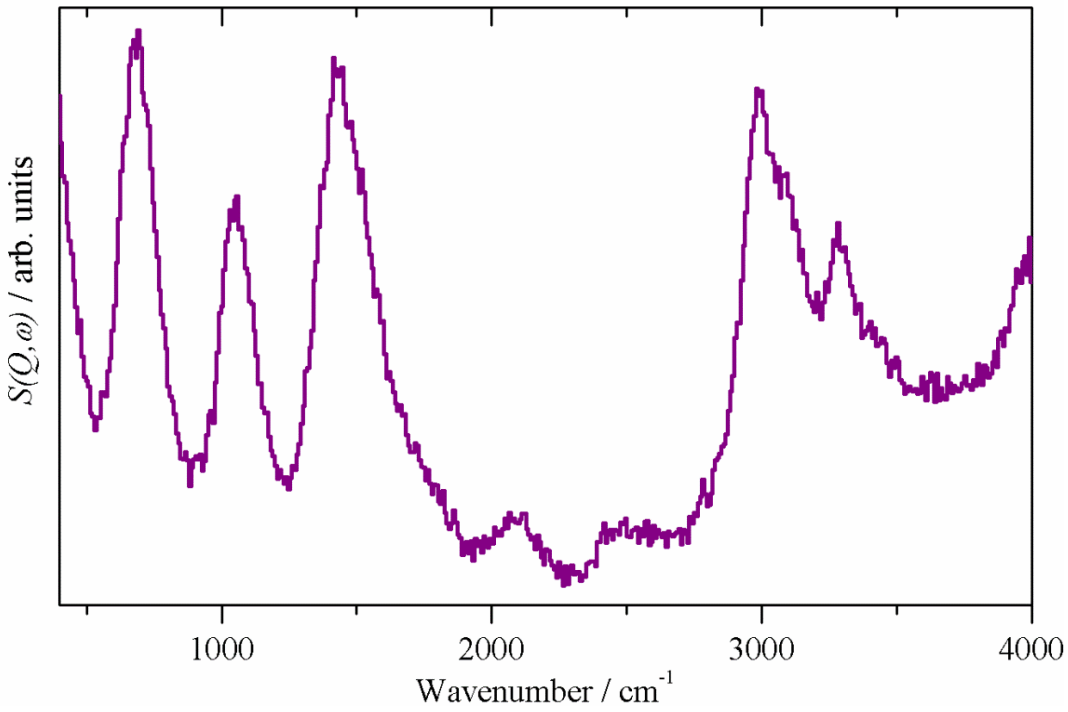

Figure 5. INS spectrum of solid propyne at 10 K recorded on MAPS with $E_i$ = 4840 $cm^{-1}$.